

# PHYSICAL REVIEW LETTERS

VOLUME 82

22 FEBRUARY 1999

NUMBER 8

## Single-Atom Interferometry

R. Huesmann, Ch. Balzer, Ph. Courteille, W. Neuhauser, and P. E. Toschek

*Institut für Laser-Physik, Universität Hamburg, Jungiusstrasse 9, D-20355 Hamburg, Germany\**

(Received 17 July 1998)

The phase shift of the hyperfine Larmor precession of an individual ground-state  $^{171}\text{Yb}^+$  ion upon pulsed variation of the ambient magnetic field has been measured by microwave-optical double resonance interpreted in terms of Mach-Zehnder interferometry. Averaging over an ensemble of *individual measurements*, compared with measurements on an ensemble of ions, demonstrates quantum ergodicity. Even a single measurement yields (incomplete) phase information. Outside the peaks and dips of the interferogram, where ion probing is incompatible with ion preparation, the results of measurements are *stochastic*. This is demonstrated by laser exciting the ion on an  $E2$  line. [S0031-9007(99)08549-X]

PACS numbers: 03.75.Dg, 32.80.Pj, 39.20.+q

One of the most sensitive and precise spectroscopic techniques is microwave-optical double resonance (MODR) [1,2], in particular when the atoms interact with spatially separated microwave fields [3]. Its variant that features instead separated *optical* signal fields has been shown to represent an atom interferometer: Only that component of the de Broglie wave which has, in fact, interacted with the light and is now ascribed to the excited state of the signal transition is affected by the light recoil and spatially separates from the ground-state component [4–7]. It has been pointed out that the states of a spin-type degree of freedom may replace spatial separation and be sufficient in order to make this scheme of atom-light interaction qualify as a Mach-Zehnder-type atom interferometer, however, in *configuration* space [8–10]. We applied microwave-optical double-resonance spectrometry to  $10^6$  laser-cooled  $^{171}\text{Yb}^+$  ions [11], confined in an electrodynamic ion trap [12,13], and to a single ion of this species [14].

Such interferometry has been extended to some 30 trapped  $^{171}\text{Yb}^+$  ions and, moreover, to an *individual* ion. Here, each measurement may yield the same result, or a random result, depending on whether the quantum evolution, after identical ion preparation, results in an ion state compatible with the detection, or not, respectively. Ramsey fringes appear in the mean rate of fluorescence detections after averaging over many *observations*. Quantum

projection noise [15] of periodically varying degrees is found superimposed upon the fringes. Opposite Larmor phase shifts applied to the upper and lower hyperfine (hf) level contributions to the ion's ground-state wave function between the two signal pulses result in a phase shift of the fringes. Restricting the averaging to smaller numbers of observation makes the projection noise increase. Individual, nonaveraged observations identify the complete microscopic state of the system: They are *selective* measurements unlike measurements on an ensemble [16]. Sequences of such measurements recorded upon certain rf detunings yield invariably “on” or “off” results, but random variations of on and off at intermediate rf frequencies. This interchange of deterministic and stochastic results is demonstrated with the rf replaced by light, i.e., by *opto*-optical double resonance (OODR) on the ion.

The experiment is made up of a 2-mm-sized trap that contains up to 50 ions. Alternatively, an individual ion is localized in the trap's electric center. Tunable frequency-doubled cw laser light at 369 nm and of 80 kHz bandwidth excites the ion(s) on the  $|S_{1/2}, F = 1\rangle \rightarrow |P_{1/2}, F = 0\rangle$  resonance line, and the scattered light is phot counted over a time interval, e.g., 2 ms. The light is down-tuned by some 20 MHz (150 MHz) in order to laser cool the ion(s). Optically pumping the ion(s) into the metastable  $^2D_{3/2}$  level is undone by illumination with 609-nm light that

retrieves the ion(s) to the ground state via the  $|D_{3/2}, F = 1\rangle \rightarrow |[1/2]_{1/2}, F = 0\rangle$  excitation. The ion is also irradiated by 12.6 GHz microwave radiation that drives the  $|S_{1/2}, F = 0, m_F = 0\rangle \rightarrow |S_{1/2}, F = 1, m_F = 0\rangle$  hyperfine transition shifted by quadratic Zeeman interaction. Optical pumping into the  $|F = 1, m_F = \pm 1\rangle$  levels is avoided when the  $E$  vector of the linearly polarized light subtends  $45^\circ$  with the direction of the dc magnetic field. A cycle of measurement (Fig. 1a) includes (i) preparing the ion in the  $|F = 0, m_F = 0\rangle$  state by a UV laser pulse that spuriously and nonresonantly excites the  $F = 1 \rightarrow 1$  transition, (ii) the first microwave  $\pi/2$  pulse, (iii) a time interval  $T$  of free evolution of the magnetic dipole, (iv) the second  $\pi/2$  pulse, and (v) probing the fluorescence by another UV pulse which simultaneously prepares the ion in the  $F = 0$  state for the next cycle. After  $N$ -fold repetition, the microwave is applied simultaneously with the UV light for recoiling the ion. Subsequent cycles involve the microwave frequency stepwise scanned across the hyperfine resonance. Figure 1b shows the interpretation of the procedure as Mach-Zehnder interferometry. Whereas the  $\pi/2$  pulses replace beam splitters, different angles of propagation are replaced by different *angles of inclination*, vs the direction of  $B$ , of the instantaneous value of the ions' magnetic moment  $\mu$ . The state of the ion(s), after the second  $\pi/2$  pulse, results from interference of two pathways of evolution. Such a Ramsey interference pattern of a *single* ion is shown in Fig. 2a, where each data point represents averaging over 40 individual observations. When, in the two "arms," i.e., in the component states, the phases are shifted differently between the two  $\pi/2$  pulses, e.g., by a pulsed variation of the ambient magnetic field, the interference pattern, although *not* the envelope, shifts in frequency (Fig. 2b).

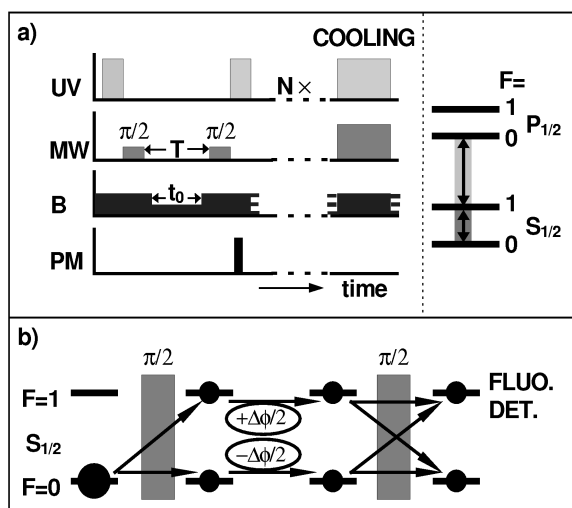


FIG. 1. (a) Gating of UV ion preparation and probe, microwave (MW), magnetic field ( $B$ ), and detector (PM). (b) Atom-wave Mach-Zehnder interferometer in configuration space. Beam splitters are replaced by  $\pi/2$  pulses.

The likeliness of finding the ion in state,  $|S_{1/2}, F = 1, m_F = 0\rangle$ , i.e., observing scattered UV light upon the final laser excitation that serves for analyzing ( $A$ ) the ion state, after preparing the ion ( $P$ ) in state  $|S_{1/2}, F = 0, m_F = 0\rangle$  initially in the cycle, is given by

$$S(\theta, \phi) = |\langle A | \mathbf{D}(\theta, \phi) | P \rangle|^2,$$

where  $\mathbf{D}$  is a composite unitary rotation of state  $P$ ,  $\theta = \sqrt{\Omega^2 + \Delta^2} \tau$  is the angle of nutation generated by a  $\tau$ -long pulse of microwave radiation,  $\Omega$  is the Rabi frequency,  $\Delta = \nu - \nu_0$ , and  $\nu$  and  $\nu_0$  are the microwave and resonance frequencies, respectively. The phase accumulated by the Larmor precession is

$$\phi = -(1/\hbar) \int \mu B dt.$$

In order to simulate a sequence of measurements on an individual ion, we first determine the pertaining amplitude, when the  $F = 1$  sublevels are nondegenerate from the field  $B \equiv B_z$  and only the transition  $F = 0 \rightarrow 1, m_F = 0 \rightarrow 0$  is excited by the signal. The operator of rotation is made up of a free precession by  $\phi$ , about  $z$ , sandwiched between two series of three rotations each, by the angles  $\chi$  about the  $x$  axis,  $\theta$  about the  $y$  axis, and  $-\chi$  about the  $x$  axis again, where  $\tan \chi = \Delta/\Omega$ , i.e., [17]

$$D_{m''m}(\chi, \theta) = \sum_{\mu\mu'=-1/2}^{1/2} d_{m''\mu'}^{(1/2)}(-\chi) d_{\mu'\mu}^{(1/2)}(\theta) d_{\mu m}^{(1/2)}(\chi),$$

such that

$$D_{m''m}(\chi, \theta, \phi) = \sum_{m'} D_{m''m'}(\chi, \theta) e^{im'\phi} D_{m'm}(\chi, \theta).$$

Here,  $m, m', m'' = +1/2$  or  $-1/2$  stand for the ion's states  $|F = 1, m_F = 0\rangle$  and  $|F = 0, m_F = 0\rangle$  at the time of preparation ( $m$ ), free evolution ( $m'$ ), and analysis ( $m''$ ), respectively. The rotations  $D$  represent the "beam

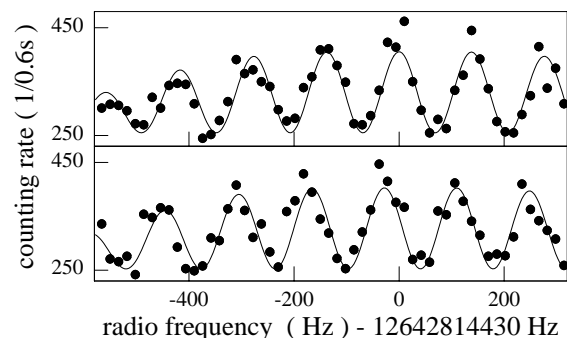


FIG. 2. Photo counting rate of single-ion fluorescence vs microwave detuning. Each data point shows accumulated results of 300 attempts; dc magnetic field  $B_0$  constant (top), and set to  $B_0 - \Delta B$ , during  $t_0$ , yielding the phase shift of fringes  $\langle \Delta \phi \rangle_{+1/2} = 1.28$  rad.

splitters" of the Mach-Zehnder scheme. The probability of finding the ion in the upper state  $+1/2$ , i.e.,  $S \equiv |f(+1/2, \theta, \phi)|^2$ , is represented by the curves fitting the data in Figs. 2a and 2b.

The expectation value of the phase of precession, when the ion has been prepared initially in  $m$ , is

$$\langle \hat{\phi}_m \rangle = \sum_{m'm''} \langle A | \mathbf{D}P \rangle \langle \mathbf{D}P | \hat{\phi} | A \rangle,$$

and the expectation value *under the condition* of final fluorescence detection is

$$\langle \hat{\phi}_{-1/2} \rangle_{m''=+1/2} = |f(+1/2, \theta, \phi)|^2 \phi / 2,$$

where the precessional phase operator is  $\hat{\phi} = \phi \hat{\sigma}_z / \hbar = -i\phi \partial / \partial \phi$  and, with a constant magnetic field  $B_0$  and  $m_F = 0 \rightarrow 0$ , we have  $\phi_0 = -\frac{1}{2} \omega_{\text{hf}} \eta^2 B_0^2 T$ . Here,  $\hat{\sigma}$  is the Pauli spin operator,  $\eta = (g_I \mu_N - g_J \mu_0) / \hbar \omega_{\text{hf}}$ , the ground-state hf splitting is  $\omega_{\text{hf}}$ , and  $g_I$ ,  $g_J$  and  $\mu_N$ ,  $\mu_0$  are the nuclear and electronic  $g$  factors and nuclear and Bohr magnetons, respectively. The phase is shifted differently along the two interferometric paths of the ion's free evolution between the  $\pi/2$  pulses: Variation of the dc magnetic field  $B_0$  by  $\Delta B$  over time interval  $t_0 \leq T$  gives rise to

$$\begin{aligned} \phi = \phi_0 + \Delta\phi = & -\frac{1}{2} \omega_{\text{hf}} \eta^2 \\ & \times [B_0^2(T - t_0) + (B_0 + \Delta B)^2 t_0], \end{aligned}$$

such that the expectation value of the phase shift after successful probing is

$$\begin{aligned} \langle \Delta\phi \rangle_{+1/2} = & |f(+\frac{1}{2}, \theta, \phi)|^2 \phi / 2 \\ & - |f(+\frac{1}{2}, \theta, \phi_0)|^2 \phi_0 / 2. \end{aligned}$$

This phase shift of fringes observed with 300 superimposed detections on an *individual* ion, as well as with individual observations on an ensemble of some 30 ions, plotted vs the Larmor phase shift  $\Delta\phi$  is shown in Fig. 3. The data represent experimental proof of the quantum version of ergodicity for the two-level system [18].

An attempt at measuring the phase on an individual particle by a single observation does not seem likely to provide any information. In fact, with such an observation, certain phase values that are possible *a priori* are excluded, and *partial* information is derived which is augmented by each follow-up observation, as will be shown. The extreme values of the emerging fringes correspond to situations where the probing of the particle state ( $F = 1$  or  $0$ , i.e.,  $m'' = +1/2$  or  $-1/2$ ) is *compatible* with the particle's preparation. Everywhere else in the fringes, in particular at the halfway values, the probing is *incompatible* (the corresponding operators  $\hat{A}$  and  $\hat{\mathbf{D}}\hat{P}$  "do not commute"). Since the detected signal of ion excitation is two-valued (1 or 0), its variance at these halfway positions gives rise to maxi-

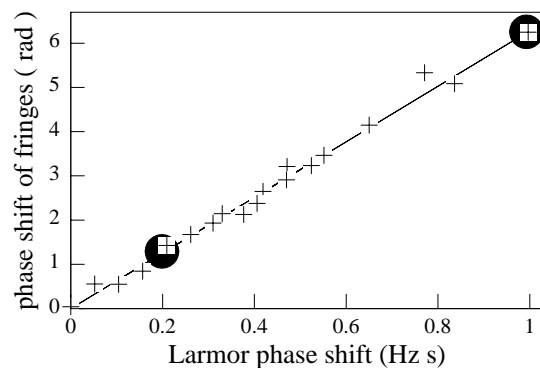


FIG. 3. Phase shift of fringes  $\langle \Delta\phi \rangle_{+1/2}$  vs Larmor phase shift  $\Delta\phi$ , for an ensemble of some 30 ions (+) and for 300 detections on *individual* ions, as in Fig. 2 (●). Variation of  $\Delta\phi$  by  $0, 5 \leq t_0 \leq 5$  ms.

imum *projection noise* [15]. In contrast, at the extreme values, no projection noise appears. Upon increasing the number of individual phase measurements whose results are lumped together for an average, the projection noise decreases. The spectral distribution of projection noise is particularly undesirable when the slope of a fringe is supposed to serve as the discriminant for the frequency control of a laser that represents a frequency standard, since for this purpose the signals at both wings of a fringe are compared in order to derive feedback for frequency reset. The distribution may be shifted by another rotation in configuration space such that the minimum variance appears at the halfway frequencies ("spin squeezing") [19].

Whereas *a priori* the probability  $P(\phi)d\phi$  of finding a particular phase value between  $\phi$  and  $\phi + d\phi$  of the ion's azimuthal wave function does not depend on that phase angle, this is not so even after a single observation of the ion in one of its  $m'' = \pm 1/2$  states:

$$\begin{aligned} P(\phi) &= (\phi/2)^{-1} \langle A, +1/2 | \hat{\phi} | A, +1/2 \rangle \\ &= 1 - (\phi/2)^{-1} \langle A, -1/2 | \hat{\phi} | A, -1/2 \rangle \\ &= \sin^2 \theta \cos^2 \frac{\phi}{2}. \end{aligned}$$

Each consecutive result of a measurement modifies this probability, and for a trajectory of  $n$  measurements at signal frequency  $\nu$ , of which  $r$  yields the fluorescence signal, the probability per unit phase is

$$\begin{aligned} P_{n,r}(\nu, \phi) &= \binom{n}{r} \sin^{2r} \theta(\nu) \cos^{2r}(\phi/2) \\ &\quad \times [1 - \sin^2 \theta(\nu) \cos^2(\phi/2)]^{n-r}. \end{aligned}$$

This evolution of the knowledge on the phase is shown in Fig. 4, where  $P_{n,n}(\nu_0)$ , the probability for the appearance of homogeneous sequences of results on resonance, is plotted, vs  $\phi$ , for various values of  $n$ . Note that with  $n \rightarrow \infty$  the fringe spectrum features a well-defined phase, lacks projection noise, and agrees with that of a measurement on a large ensemble.

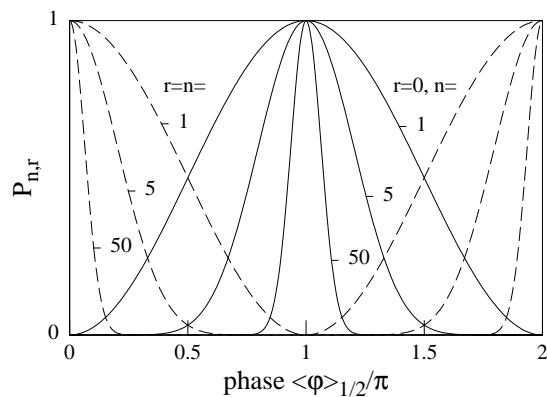


FIG. 4. Probability  $P_{n,r}$  of finding phase  $\langle \phi \rangle_{1/2}$  of Ramsey fringes upon  $r$  results (out of  $n$  accumulated attempts) showing resonance scattering. Note that even a single observation restricts the range of possible phase values.

MODR on the ground-state hyperfine transition of a single  $^{171}\text{Yb}^+$  ion suffers from low efficiency of the cyclic fluorescence excitation on the line  $|S_{1/2}, F = 1, m_F = 0\rangle \rightarrow |P_{1/2}, F = 0, m_F = 0\rangle$  which is bypassed by spurious scattering in the wing of the line  $|S_{1/2}, F = 1\rangle \rightarrow |P_{1/2}, F = 1\rangle$  and concomitant pumping the ion into the  $|S_{1/2}, F = 0\rangle$  level. Consequently, averaging over some twenty individual measurements at each value of signal detuning has been required in order to display a spectrum. In contrast, interruption of fluorescence by excitation of the  $E2$  line at 411 nm that takes the ion into its  $D_{5/2}$  level (OODR) is efficient and displays “quantum amplification.” Trajectories of gated detections of light scattering alternating with driving the ion on the  $E2$  transition (but with initial preparation not repeated) show stochastic series of on and off detection (Fig. 5) and the concomitant “quantum jumps” [20,21]. However, at periodic light frequencies, the results are predetermined owing to *coherent* interaction of the ion with the radiation field, and the results on or off are *certain* at nutation angles  $\theta(\nu)$  that are multiples of  $\pi/2$ . From the spectrally alternating deterministic and stochastic results, the phase of the Ramsey fringes may be derived by determining the spectral periodicity from second-order spectral correlation and fitting the phase. Consequently, although for the full determination of the phase an ensemble of measurements is indispensable, this ensemble need not consist of measurements under equal conditions.

In conclusion, atom interferometry has been extended to an individual atomic particle, a trapped and cooled  $^{171}\text{Yb}^+$  ion. The phases of the wave functions responsible for the Larmor precession of the coupled electronic and nuclear magnetic moments are separately addressed in the arms of a Mach-Zehnder-like arrangement, and they have been shifted in opposite directions by a pulsed variation of the ambient magnetic field. The variation of the magnetic potential felt by the ion’s induced magnetic moment gives

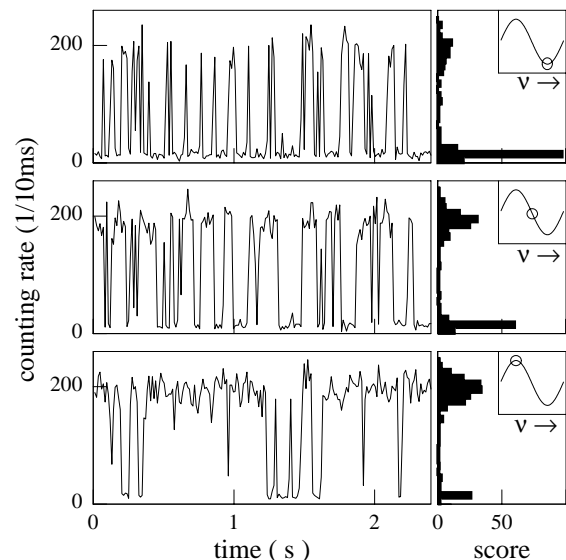


FIG. 5. Photocounting rate of  $^{172}\text{Yb}^+$  single-ion resonance scattering after an attempted laser excitation on  $S_{1/2}-D_{5/2}$   $E2$  line, at laser detuning to dip (top), midslope (center), and peak of fringe (bottom) shown in the insets. Distributions of counting rates (right-hand graphs) correspond to deterministic (top, bottom) and stochastic (center) measurements. Spurious counts in the upper score and “no counts” in the lower one are caused by imperfections in the frequency setting.

rise to a shift of the observed fringes as known from the scalar Aharonov-Bohm effect. From a series of results of *individual* measurements, a phase distribution with a most probable phase may be determined. This probability distribution becomes narrowed upon each individual measurement reiterated, such that the phase of the fringes becomes better defined with the number of measurements increasing. Spectro-temporal series of *individual* measurements alternate, upon scanning, between deterministic and stochastic results, as shown by OODR on an  $E2$  line.

P.E.T. acknowledges discussions with D. Reiss and information from F. Haake and B. Eckhardt. This work was supported by the Körber-Stiftung, Hamburg, by the Hamburgische Wissenschaftliche Stiftung, and by the ZEIT-Stiftung, Hamburg.

\*Email address: toschek@physnet.uni-hamburg.de

- [1] J. Brossel and F. Bitter, Phys. Rev. **86**, 308 (1952).
- [2] A. Kastler and J. Brossel, C.R. Acad. Sci. **229**, 1213 (1949).
- [3] N.F. Ramsey, Phys. Rev. **76**, 996 (1949).
- [4] F. Riehle, A. Witte, T. Kisters, and J. Helmcke, Appl. Phys. B **54**, 333 (1992).
- [5] C.J. Bordé, Phys. Lett. A **140**, 10 (1989).
- [6] K. Zeiske, G. Zinner, F. Riehle, and J. Helmcke, Appl. Phys. B **60**, 205 (1995).
- [7] J.H. Müller, D. Bettermann, V. Rieger, K. Sengstock, U. Sterr, and W. Ertmer, Appl. Phys. B **60**, 199 (1995).

- [8] K. Sangster, E. A. Hinds, S.M. Barnett, and E. Riis, *Phys. Rev. Lett.* **71**, 3641 (1993).
- [9] S. Nic Chormaic *et al.*, *Phys. Rev. Lett.* **72**, 1 (1994).
- [10] A. Görlitz, B. Schuh, and A. Weis, *Phys. Rev. A* **51**, R4305 (1995).
- [11] R. Casdorff, V. Enders, R. Blatt, W. Neuhauser, and P.E. Toschek, *Ann. Phys. (Leipzig)* **48**, 41 (1991).
- [12] W. Paul, O. Osberghaus, and E. Fischer, *Forschungsber. Wirtsch. Verkehrsministeriums NRW, Series 415* (1955); E. Fischer, *Z. Phys.* **156**, 1 (1959).
- [13] P.E. Toschek, in *New Trends in Atomic Physics*, Proceedings of the Les Houches Summer School, Session XXXVIII, edited by G. Grynberg and R. Stora (North-Holland, Amsterdam, 1984), p. 385.
- [14] V. Enders, Ph. Courteille, R. Huesmann, L.S. Ma, W. Neuhauser, R. Blatt, and P.E. Toschek, *Europhys. Lett.* **24**, 325 (1993).
- [15] W.M. Itano, J.C. Bergquist, J.J. Bollinger, J.M. Gilligans, D.J. Heinzen, F.L. Moore, M.G. Raizen, and D.J. Wineland, *Phys. Rev. A* **47**, 3554 (1993).
- [16] M.J. Gagen and G.J. Milburn, *Phys. Rev. A* **47**, 1467 (1993).
- [17] See, e.g., A.R. Edmonds, *Angular Momentum in Quantum Mechanics* (Princeton University, Princeton, NJ, 1960).
- [18] Matrix elements, in the semiclassical limit, approach the microcanonical average. See M. Feingold and A. Peres, *Phys. Rev. A* **34**, 591 (1986).
- [19] D. Wineland, J.J. Bollinger, W.M. Itano, and D.J. Heinzen, *Phys. Rev. A* **50**, 67 (1994).
- [20] W. Nagourney, J. Sandberg, and H. Dehmelt, *Phys. Rev. Lett.* **56**, 2797 (1986).
- [21] Th. Sauter, W. Neuhauser, R. Blatt, and P.E. Toschek, *Phys. Rev. Lett.* **57**, 1696 (1986).